Angular dependence and interfacial roughness in exchange-biased ferromagnetic/antiferromagnetic bilayers

Joo-Von Kim and R. L. Stamps
Department of Physics, The University of Western Australia, Nedlands WA 6907, Australia

B. V. McGrath and R. E. Camley
Department of Physics, The University of Colorado at Colorado Springs, Colorado Springs, Colorado 80933-7150

(Received 12 October 1999)

A theoretical study of the angular dependence of exchange bias in coupled ferromagnetic/antiferromagnetic bilayers is presented. The variation of the bias field with applied field angle is shown to be strongly affected by the canting of the interfacial spins, particularly with the presence of defects. Discontinuities in the angular dependence of the bias field are found to depend on the sense of rotation of the ferromagnetic layer upon reversal.

I. INTRODUCTION

Exchange bias has been a subject of intense interest because of its applications in field-sensor devices.[1] Exchange bias[2] results from exchange coupling between ferromagnetic and antiferromagnetic layers, and is characterized by a displacement of the hysteresis loop along the field axis. This effect is established in an experimental system when the interfacial ferromagnetic and antiferromagnetic spins are preferentially ordered, either by field cooling the sample through the Néel temperature (T_N) of the antiferromagnet or by antiferromagnetic deposition on a cold ferromagnet substrate. In either case, the ferromagnetic layer is prepared to be a single domain state. In general, the Curie temperature of the ferromagnetic layer (T_C) is larger than T_N, although recent experimental studies have investigated the uncommon situation where $T_C < T_N$.[3] Both the bias field and the coercivity decrease as temperature increases, disappearing above the blocking temperature (T_B) of the antiferromagnet, where $T_B \leqslant T_N$ in general. This confirms that the antiferromagnetic order plays a crucial role in this mechanism. The center of the hysteresis loops are usually displaced in the negative field direction, although experiments have also shown the possibility for positive bias.[4,5]

The original model proposed by Meiklejohn and Bean[6,7] is based on a perfect uncompensated interface between the ferromagnetic and antiferromagnetic layers, where the interfacial antiferromagnetic spins possess a net magnetic moment and ferromagnetic alignment across the interface is assumed. Bias field estimates from this model require a large uniaxial anisotropy in the antiferromagnetic layer and are proportional to the coupling strength across the interface. The uniaxial anisotropy in the antiferromagnetic layer introduces a unidirectional anisotropy in the ferromagnetic layer through exchange coupling. However, this model predicts values of the bias field H_E that are two orders of magnitude too large.[8,9] Mauri *et al.*[10] and Koon[12] have shown that the formation of an antiferromagnetic domain wall perpendicular to the interface during magnetization reversal can lead to exchange bias, giving correct order of magnitude estimates for the bias field. Their models also predict a minimum antiferromagnetic layer thickness for exchange bias, governed by the spatial dimensions required to support such a domain wall—features verified experimentally.[13,14] Koon also demonstrated that compensated interfaces, where the net antiferromagnetic moment is zero, can also support exchange bias and results in a perpendicular coupling of the ferromagnetic moment to the anisotropy axis, reminiscent of the spin-flop transition in antiferromagnetic materials with uniaxial anisotropy.

Most theoretical studies have been devoted to explaining the origin and magnitude of the bias field H_E. However, other features characteristic of exchange bias systems have only been studied in the experimental domain. An important aspect is the directional properties of exchange bias. The angular dependence of H_E and the coercivity H_C was first explored experimentally in NiFe/CoO bilayers.[15] The system was field cooled along a chosen axis and hysteresis loop measurements were then taken along different angles relative to the initial direction. The variations obtained in H_E and H_C as a function of the field angle θ_H were not simple sinusoidal functions as initially expected.[6,7] The experimental results can be better described with cosine series expansions, with odd and even terms for H_E and H_C, respectively, due the unidirectional and uniaxial nature of the corresponding energies. The complicated angular behavior results in larger contributions from higher-order $a_n \cos n\theta_H$ terms relative to the base $a_1 \cos \theta_H$ term. Similar results have been obtained in studies on monocrystalline and polycrystalline structures,[16,17] where the presence of a fourfold anisotropy has been shown to affect $H_E(\theta_H)$ significantly. However, experiments with amorphous[18] and permalloy[19] ferromagnetic layers display a simpler angular dependence.

The paper is organized as follows. In Sec. II, we outline an analytical model based on a perfect uncompensated interface to study the angular dependence of H_E. In Sec. III, we present a numerical model to examine the effects of nonuniformities in the spin system, particularly the role of interfacial defects. We also investigate the importance of the preparation of the initial state. Finally, a discussion and

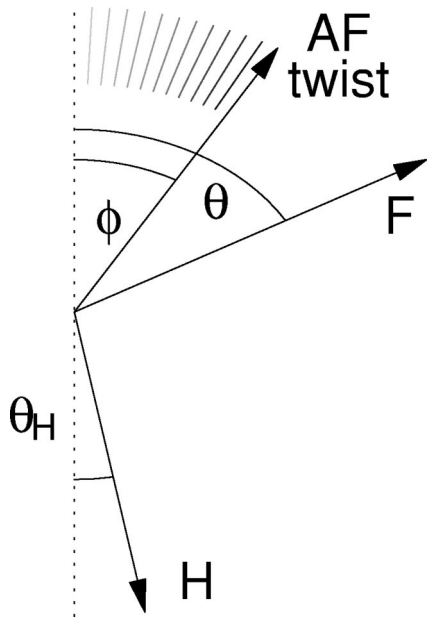

FIG. 1. Simple model of a perfect uncompensated interface used to estimate the magnitude of the bias field. A twist in the antiferromagnetic layer is formed upon the reversal of the ferromagnetic layer.

concluding remarks are presented in Sec. IV.

II. ANALYTICAL RESULTS

An analytic estimate of the bias field can be derived as follows. Consider a perfect uncompensated interface between the ferromagnet/antiferromagnet bilayer (Fig. 1), where both layers are assumed to be single domain. The free energy of the system is

$$\varepsilon=\sigma_t-J_I\cos(\theta-\phi)+M_FHt_F\cos(\theta+\theta_H), \tag{1}$$

where σ_t is the energy of the antiferromagnetic twist formed, the second term is the exchange-coupling energy between the ferromagnetic and antiferromagnetic layers, and the third term represents the Zeeman energy of the ferromagnetic layer in an applied field H. J_I is the exchange coupling energy across the interface between the ferromagnetic and antiferromagnetic layers. M_F and t_F are the magnetization per unit surface area and thickness of the ferromagnetic layer, respectively. The antiferromagnetic twist is initiated by the reversal of the ferromagnetic layer, and arises from the competition between the following energies: (1) The exchange coupling energy between the interfacial ferromagnetic and antiferromagnetic spins; (2) The exchange energy in the antiferromagnet; (3) The uniaxial anisotropy energy in the antiferromagnet. To derive the energy of the twist, we first consider the total energy of a domain wall. This energy is given by

$$\sigma_t=\int_{-\infty}^{\infty}\left[A\left(\frac{\partial\Phi(z)}{\partial z}\right)^2+K_u\sin^2\Phi(z)\right]dz, \tag{2}$$

where we have assumed a continuum chain of spins along the z axis.[10,11] The angle of these spins relative to the anisotropy axis perpendicular to the z axis is denoted by $\Phi(z)$. The first term describes the exchange energy between neighboring spins in the antiferromagnet, with A denoting the strength of the exchange stiffness. The second term in the integrand describes the local anisotropy energy of a spin at position z of strength K_u. This domain wall energy is minimized by solving the Euler-Lagrange equation for Eq. 2. The solution $\Phi_0(z)$ is

$$\Phi_0(z)=2\arctan\left[e^{-\kappa z}\tan\left(\frac{\phi}{2}\right)\right], \tag{3}$$

where ϕ is the angle of the interfacial spin relative to the anisotropy axis. The twist energy is obtained upon substitution of Eq. (3) into Eq. (2),

$$\sigma_t=2\sqrt{AK_u}[1-\cos(\phi)]. \tag{4}$$

With this expression, we minimize the total energy (1) with respect to θ and ϕ to give the following conditions:

$$\tan(\theta)=\frac{J_I\sin(\phi)+M_FHt_F\sin(\theta_H)}{J_I\cos(\phi)-M_FHt_F\cos(\theta_H)}, \tag{5}$$

$$\tan(\phi)=\frac{J_I\sin(\theta)}{2\sqrt{AK_u}+J_I\cos(\theta)}. \tag{6}$$

For a reversible magnetization (M vs H) curve, the bias field is defined as the zero of that curve [i.e., $M(H_E)=0$], and is obtained by imposing the requirement that $\theta+\theta_H=90°$. The following expression results:

$$H_E=\frac{J_I}{M_Ft_F}\frac{\cos\theta_H}{\sqrt{\gamma^2+\gamma|\sin\theta_H|+1}}, \tag{7}$$

where the quantity

$$\gamma=\frac{J_I}{2\sqrt{AK_u}} \tag{8}$$

represents a ratio between the interlayer coupling energy and the antiferromagnetic domain wall energy.

In the rigid coupling limit of large γ (i.e., $J_I\gg2\sqrt{AK_u}$), the formation of a domain wall in the antiferromagnetic layer is preferred upon the reversal of the ferromagnet. The bias field is then independent of J_I,

$$H_E=\frac{2\sqrt{AK_u}}{M_Ft_F}\cos\theta_H. \tag{9}$$

In the other limit $\gamma\to0$, where the interlayer coupling energy is much less than that of the antiferromagnetic domain wall, the angular dependence is simply proportional to J_I,

$$H_E=\frac{J_I}{M_Ft_F}\cos\theta_H. \tag{10}$$

For the $\theta_H=0°$ case these limiting forms give Mauri's expression (9), and Meiklejohn and Bean's expression (10). In both of these limits, the angular dependence of the bias field is a simple sinusoidal function. A more complicated angular dependence only arises when γ is of order unity, i.e., when the domain wall energy and the interlayer exchange energy

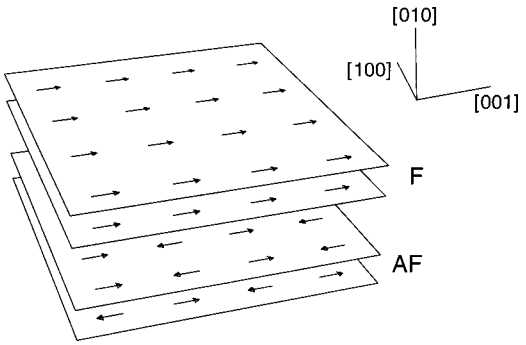

FIG. 2. Geometry of the numerical model for a system with a compensated interface.

are comparable. In this regime, the interfacial spins experience greater canting, similar to that found in the bulk antiferromagnetic spin-flop state.

III. NUMERICAL RESULTS

A. Model

We employ a numerical method to determine the microscopic spin configuration that should appear in a realistic structure. The ferromagnet/antiferromagnet bilayer is modeled as a simple cubic structure, with nearest-neighbor exchange interactions along the cube edges (Fig. 2). A Heisenberg Hamiltonian is used,

$$\mathcal{H}=-g\mu_0\mu_B\sum_i \mathbf{H}\cdot\mathbf{S}_i-\sum_{i,j} J_{ij}\mathbf{S}_i\cdot\mathbf{S}_j+K_0\sum_i (S_{iy})^2 + K_u\sum_i (S_{iz})^2, \tag{11}$$

where the spin operators are treated as vector quantities. The summation over the index i represents a sum over all spins in the system, while j denotes a sum over the nearest neighbors. The first term is the Zeeman term, where g is the Landé factor, μ_0 is the permeability of free space, and μ_B is the Bohr magneton. The second term is the exchange term. The third term describes a planar anisotropy that favors spin rotation in the (010) plane. The final term represents a uniaxial crystalline anisotropy in the antiferromagnet along the z axis, where S_{iz} denotes the z component of the ith spin. The semiclassical limit is considered where $\mathbf{S}$ is a vector that can rotate freely into any direction. It is assumed that J_{ij} is constant across the interface and within the ferromagnetic and antiferromagnetic bulk. The interlayer exchange coupling is denoted by J_I, the ferromagnetic exchange energy by J_F and the antiferromagnetic exchange energy by J_{AF}. Periodic boundary conditions are applied in the [100] and [001] directions, so we only have to consider the motion of a single (100) plane of spins. All applied fields are constrained to lie in the (010) plane.

The equilibrium configuration is found as follows. The local field $\mathbf{h}_i$ at site i is calculated first according to $\mathbf{h}=-\nabla_s\mathcal{H}$,

$$\mathbf{h}_i=\mathbf{H}+\frac{1}{g\mu_0\mu_B}\left(\sum_j J_{ij}\mathbf{S}_j+2K_0S_{iy}\hat{\mathbf{y}}+2K_uS_{iz}\hat{\mathbf{z}}\right). \tag{12}$$

A local energy minimum is attained when $\mathbf{S}_i$ is aligned in parallel with $\mathbf{h}_i$. The Landau-Lifshitz equation is used to describe the time-dependent spin relaxation into the local field direction

$$\frac{d\mathbf{S}_i}{dt}=-\gamma_g\mathbf{S}_i\times\mathbf{h}_i+\alpha\mathbf{S}_i\times\mathbf{S}_i\times\mathbf{h}_i. \tag{13}$$

The first term represents the precessional motion of the magnetization, which moves in a direction perpendicular to both $\mathbf{S}$ and $\mathbf{h}$. The second term represents motion perpendicular to both $\mathbf{S}$ and $\mathbf{S}\times\mathbf{h}$ that acts to damp the precessional motion. Here, γ_g is the gyromagnetic constant and the coefficient α is related to the relaxation frequency which is a measure of the degree of damping.

To obtain the equilibrium configuration for the spin array, the system of equations (13) is solved by numerical integration using a second-order Runge-Kutta method. Unless otherwise specified, the following ratios are used: $J_F/K_u=100$, $J_{AF}/K_u=-10$, $J_I/K_u=-30$, and $K_0=K_u$. No uniaxial anisotropies are present in the ferromagnetic layer, but an easy plane anisotropy is included in both ferromagnetic and antiferromagnetic layers. The thicknesses of the ferromagnetic and antiferromagnetic layers are 10 and 15 monolayers, respectively. All field values are quoted in units of $K_u/(g\mu_0\mu_B)$, with $H=H'g\mu_0\mu_B/K_u$, with H' given in A/m.

To calculate the magnetization curve, we employ the following procedure. (1) The direction of the spins are randomized. (2) The equilibrium configuration of the system is determined in the presence of a $H=40$ field, applied at an angle θ_{cool} relative to the antiferromagnet anisotropy axis. (3) H is decreased to zero over several increments, with the equilibrium configuration calculated at each increment. (4) A magnetization curve is then calculated for a field applied at θ_H relative to the antiferromagnet axis.

B. Perfect interfaces

The angular dependence of H_E is first examined for an uncompensated system with $\theta_{\text{cool}}=0°$. This cooling direction is chosen to coincide with the antiferromagnet anisotropy axis. The external field angle θ_H is varied between 0° and 360° in increments of 10°. For each field increment, we obtained a reversible magnetization curve with zero coercivity. Hence, the value of the bias field H_E for each case is determined by simply calculating the zero of $M(H)$. Following Ambrose *et al.*,[15] the function $H_E(\theta_H)$ we obtained is expanded in a $\cos n\theta_H$ series, where n is odd to reflect the unidirectional nature of exchange bias. The best fit to our numerical results is given by

$$H_E=0.457(\cos\theta_H+0.019\cos 3\theta_H+\cdots) \tag{14}$$

showing that contributions from higher order terms only amount to $\approx 2\%$. For the compensated system, the ferromagnetic spins were observed to couple preferentially in a perpendicular direction to the antiferromagnet anisotropy axis, as described by Koon.[12] In this case, the cooling field was applied at 90°, corresponding to the maximum in H_E that is

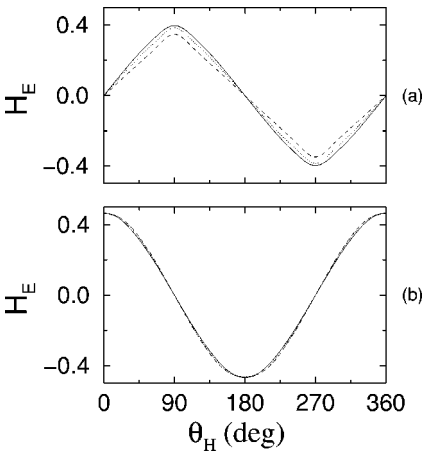

FIG. 3. $H_E(\theta_H)$ with $J_I/K_u=-30$ (—), -40 ($\cdots$), and -50 ($--$), for (a) compensated and (b) uncompensated interfaces. The bias field H_E is in units of $K_u/(g\mu_0\mu_B)$.

expected to occur at this angle. A sine series expansion is therefore more appropriate, with a fit to the numerical results being

$$H_E=0.364(\sin\theta_H-0.058\sin 3\theta_H+0.017\sin 5\theta_H+\cdots). \tag{15}$$

Here, the contribution from higher order terms is roughly three times larger at $\approx 6\%$. The angular dependence is clearly affected by the interfacial spin orientations; the spin-flop state induced by the perpendicular coupling between the ferromagnetic and antiferromagnetic layers leads to a large degree of nonuniform canting experienced by the interfacial antiferromagnetic spins. This in turn results in a more complicated form for $H_E(\theta_H)$, as predicted by our analytical work described earlier.

To further examine the effects of interfacial spin canting, $H_E(\theta_H)$ is studied as the strength of J_I is varied. The cooling angles are the same as those used above. Canting of the interfacial spins is sensitive to J_I, and is most pronounced at the compensated interface where the spins of one sublattice cant differently to the spins of the other. The calculated angular curves for H_E are presented in Fig. 3. The following cases are considered for both interfaces: $J_I/K_u=-30,-40$, and -50. For the compensated interface, there is a slight decrease in the maximum of H_E as J_I is increased. The spin-flop configuration of the antiferromagnet results in a net antiferromagnetic moment antiparallel to the ferromagnet spins. The magnitude of the net AF moment increases as J_I is increased. Upon the reversal of the ferromagnetic layer for increasing J_I, it is observed that the extent of the AF twist formed decreases, which results in a smaller bias field.

For the uncompensated interface [Fig. 3(b)], variations in the magnitude of the bias field maxima and the curvature of $H_E(\theta_H)$ are less significant. For this interface, increases in the interlayer coupling result in less canting, as all interfacial spins are preferentially aligned in antiparallel. Note that this behavior is not represented by a biquadratic term assumed recently in some treatments.[20,21]

C. Rough interfaces

Defects are simulated by mixing both ferromagnetic and antiferromagnetic spins at the interface. This is shown in the cross-sectional diagram of Fig. 4. A single site defect in Figs. 4(a) and 4(b) is referred to as a line defect since the periodic boundary conditions in the [001] direction ensure that the defect is repeated in each unit cell in the [001] direction. We also examine results for a step defect where two or more defects are introduced as shown in Figs. 4(c) and 4(d). For simplicity only defects of one atomic height are considered. Note that the spin configurations depicted in Fig. 4 are schematic, and do not represent calculated orientations.

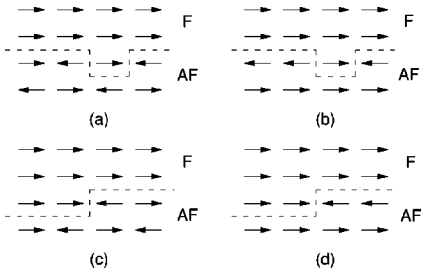

FIG. 4. Schematic diagram showing line defects [(a) and (b)] and step defects [(c) and (d)] at compensated and uncompensated interfaces, respectively.

Introducing a line defect in a compensated surface creates an asymmetry between the number of ''up'' and ''down'' spins at the interface. We can study the impact of this asymmetry by plotting the ''natural'' angle of the ferromagnet $\theta_{\rm nat}$ measured relative to the antiferromagnet anisotropy axis, for different sizes of the unit cell in the [001] direction (Fig. 5). This size is denoted by Λ. The angle $\theta_{\rm nat}$ is determined by calculating the equilibrium orientation of the ferromagnet spins from an initial randomized state, in the absence of an applied field.[22] A large exchange energy in the ferromagnetic layer is present so that all ferromagnet spins are aligned parallel. The largest asymmetry occurs for $\Lambda=2$ where only one antiferromagnet sublattice spin is present at the interface. This is uncompensated like in behavior and results in $\theta_{\rm nat}=0°$. In the limit of a perfect interface $\Lambda\to\infty$, the ratio of the antiferromagnet sublattice interfacial spins become nearly equal and results in the tendency $\theta_{\rm nat}\to 90°$. For the uncompensated case, an opposite trend is observed with a compensated like interface at $\Lambda=2$ ($\theta_{\rm nat}=90°$) and $\theta_{\rm nat}\to 0°$ as $\Lambda\to\infty$.

The natural angle defines an axis along which a magnetization curve measurement attains the largest value of H_E, since this is the equilibrium orientation of the ferromagnetic layer. The natural angles for the perfect compensated and

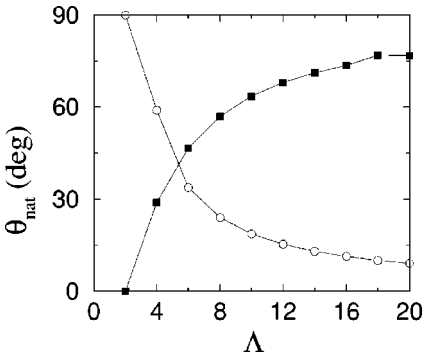

FIG. 5. The natural angle $\theta_{\rm nat}$ as a function of defect spacing Λ, for compensated ($-\blacksquare-$) and uncompensated ($-\bigcirc-$) interfaces.

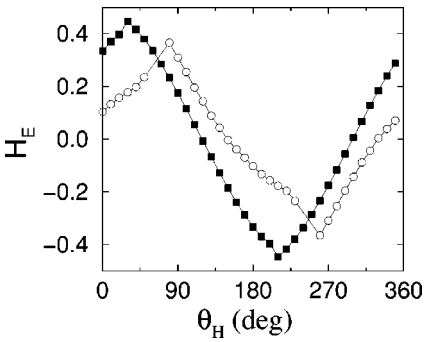

FIG. 6. $H_E(\theta_H)$ for a compensated ($-\blacksquare-$) and an uncompensated ($-\bigcirc-$) system with line defects ($\Lambda=4$). The bias field H_E is in units of $K_u/(g\mu_0\mu_B)$.

uncompensated interfaces are 90° and 0°, respectively. Note that this is only true at 0 K; we show elsewhere[22] that $\theta_{\rm nat}$ is strongly dependent on temperature. The presence of asymmetry in the antiferromagnet sublattice spins at the interface leads to a bifurcation in the natural angle at 0°, in this case the axes for $H_{E,\max}$ are defined by $\pm\theta_{\rm nat}$. This splitting in the equilibrium orientation results from the $\sin^2\theta$ term in the uniaxial anisotropy, which gives the possibility for two unique solutions. In the case of the $\Lambda=4$ line defect at the uncompensated interface, $\theta_{\rm nat}\approx 60°$, so the equilibrium orientation of the ferromagnetic spins can assume either of the energetically equivalent states $\approx 60°$ or $\approx -60°$. In Fig. 6, we plot the variation of H_E with θ_H for a line defect with $\Lambda=4$ for both interfaces. It is immediately apparent that the minima and maxima of $H_E(\theta_H)$ have been shifted along the θ_H axis. The maximum value for H_E occurs at the natural angle calculated in Fig. 5.

The presence of a line defect introduces a discontinuity in the angular curves. The function $H_E(\theta_H)$ appears to be comprised of two separate branches: a ''descending'' branch for $\theta_{\rm nat}<\theta_H<\theta_{\rm nat}+180°$ and an ''ascending'' branch for $\theta_{\rm nat}-180°<\theta_H<\theta_{\rm nat}$, with the discontinuity taking place at $\theta_{\rm nat}$. This is a result of the sense of rotation of the ferromagnetic spins, as illustrated in Fig. 7. We suppose that the coupling between the interfacial ferromagnetic and antiferromagnetic spins is rigid, and we consider the magnetization processes at an uncompensated interface for simplicity. For the case where $0°<\theta_H<\theta_{\rm nat}$, the ferromagnet rotates towards the $\theta_{\rm nat}$ axis upon reversal [Fig. 7(a)]. This process becomes more favorable as the ferromagnetic spins rotate towards an equilibrium orientation corresponding to an energy minimum. The resulting reversal process is executed in a clockwise direction, causing the interfacial antiferromagnetic spins to twist by an angle ϕ_1 from the anisotropy axis [Fig. 7(b)].

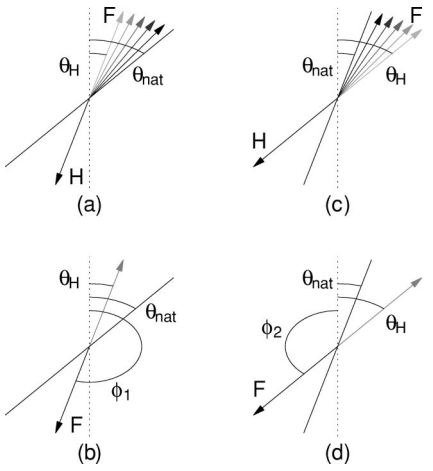

FIG. 7. The clockwise rotation (a) of the reversal of the ferromagnetic layer creates an antiferromagnetic twist with an interfacial angle of ϕ_1 (b). For the counterclockwise rotation (c), an antiferromagnetic twist with an interfacial angle of ϕ_2 is created (d). In general, $\phi_1\neq\phi_2$, resulting in the discontinuity of H_E seen in Fig. 6.

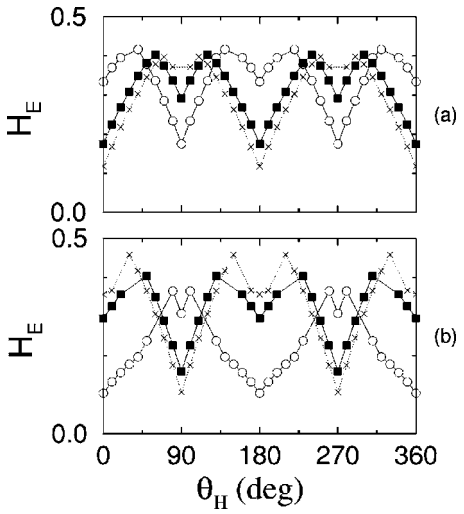

FIG. 8. $H_E(\theta_H)$ with multiple field cooling for (a) compensated and (b) uncompensated interfaces. Interfacial line defects are present with $\Lambda=4$ ($-\bigcirc-$), 8 ($-\blacksquare-$), and 12 ($-\times-$). The bias field H_E is in units of $K_u/(g\mu_0\mu_B)$.

For the other case where $\theta_H>\theta_{\rm nat}$, the ferromagnetic spins again rotate towards the $\theta_{\rm nat}$ axis for the same reason [Fig. 7(c)]. However, the reversal takes place in a counterclockwise direction and the interfacial antiferromagnetic spins are rotated through an angle of ϕ_2 [Fig. 7(d)]. It is evident that the equality $\phi_1=\phi_2$ will not hold in general for equal $|\theta_H-\theta_{\rm nat}|$. Thus, the magnitude of H_E will not be equal in magnitude for the two cases as it is dependent on the twist angle ϕ in the antiferromagnet.

D. Multiple field cooling

In this section, we study the effects on exchange bias of field cooling along different directions $\theta_{\rm cool}$. We introduce the constraint $\theta_H=\theta_{\rm cool}$, so that the field cooling and magnetization curve measurement procedures are essentially one process. By this we mean that the magnetization curve calculations do not begin from the zero-field state; the curve is calculated as H is reduced from saturation and reversed along $\theta_{\rm cool}$, so that the system is essentially field cooled at each field angle.

In Fig. 8, $H_E(\theta_H)$ is plotted for a line defect with $\Lambda=4$, 8, and 12 for both compensated and uncompensated interfaces. The striking feature of the angular curves is the appearance of four maxima over the same range of θ_H considered previously. The angles at which these maxima occur are $\theta_H=\pm\theta_{\rm nat}$ and $\theta_H=180°\pm\theta_{\rm nat}$, corresponding to the equilibrium orientation of the ferromagnetic spins as discussed earlier. In addition, $H_E\geqslant 0$ over the entire range of θ_H.

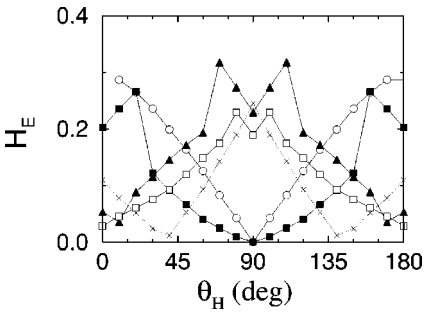

FIG. 9. $H_E(\theta_H)$ with multiple field cooling for uncompensated interfaces. Interfacial step defects are present with $\Lambda=2$ ($-\bigcirc-$), 4 ($-\blacksquare-$), 8 ($-\times-$), 16 ($-\blacktriangle-$), and 32 ($-\square-$). The bias field H_E is in units of $K_u/(g\mu_0\mu_B)$.

These features are due to the multiple field-cooling procedure. By starting the system in a saturated configuration and measuring the magnetization curve such that $\theta_H=\theta_{\text{cool}}$, only points within the range $0°<\theta_H<90°$ are unique and the period of the curves is 180°. This is due to uniaxial anisotropy in the antiferromagnetic layer which is symmetric about $\theta_H=0°$ between $-90°$ and 90°, and it follows that $H_E\geqslant 0$ always. The $\Lambda=4$ curves in Fig. 8 may be obtained from those in Fig. 6, by considering $H_E(\theta_H)$ over the range $0°<\theta_H<90°$ and performing the operation $H_E(\beta)=H_E(-\beta)$, where $\beta=\theta_H+90°$, to determine the function over the full period.

In Fig. 9, we present the results from applying the multiple field-cooling procedure to a stepped uncompensated interface with varying unit cell size Λ. In each case, the step transition is chosen to take place in the center of the unit cell (Fig. 4). The angular curves are similar to those obtained in Fig. 8 and may be analyzed in an identical manner. It is evident that the introduction of defects can greatly affect the angular dependence. The simple cosine form is suppressed and higher order terms appear.

IV. DISCUSSION AND CONCLUSION

In the numerical model presented, we have assumed an in-plane anisotropy term in the Hamiltonian (11) that prefers an in-plane rotation of the spins. This term was included to stabilize the formation of the antiferromagnetic domain wall as the ferromagnetic layer is reversed. Previous theoretical studies[23] have shown that the occurrence of exchange bias can be quite sensitive to this parameter, particularly due to the effects of thermal fluctuations. For large easy-plane fluctuations in certain cases, the creation of an antiferromagnetic twist is not favored energetically as the ferromagnetic layer is reversed. Instead, the path of rotation adopted by the ferromagnetic spins is out of plane, resulting in an irreversible process and thus a symmetric hysteresis loop about $H=0$. In the model discussed here, it was assumed that the spins remained in-plane due to a large out-of-plane anisotropy in the antiferromagnet.

It is often supposed that the strength of the interlayer coupling J_I is equal to the bulk antiferromagnet exchange energy J_{AF}, although an exact estimate has yet to be determined experimentally. In our calculations, we have chosen a ratio of $J_I/J_{\text{AF}}=3$ for computational ease. More precisely, the width of a domain wall is roughly $\pi\sqrt{|J_{\text{AF}}|/K_u}$, so the chosen parameter ratio of $J_{\text{AF}}/K_U=-10$ allows for an antiferromagnetic domain wall to be supported within $t_{\text{AF}}=15$ ML. For the compensated geometry, the formation of the antiferromagnetic wall during the reversal of the ferromagnet requires a larger value of J_I. A larger domain wall may be facilitated by a thicker antiferromagnetic layer, and exchange bias may be achieved with more realistic interlayer coupling strengths.

In Sec. III, we discussed the effects of interfacial roughness in the form of periodic line and step defects. The values of Λ chosen are small but on the order of a domain wall width. The ferromagnetic wall width is very large in these calculations so the different AF domains are coupled to the ferromagnet in the same direction everywhere. The results here show how the bias behaves as the scale of the roughness approaches the natural length scale of the antiferromagnet. For the system considered here, the domain wall width in the antiferromagnet is $\approx$10 ML, and beyond this length the defects are isolated. If the ferromagnet wall width was on the order of the roughness spacing, ferromagnetic domains could form and these results would not apply. In practice, the field-cooling direction defines the unidirectional axis of exchange bias, and hysteresis loops are measured at different angles relative to this axis. In most cases, the antiferromagnetic layers are multigrained structures that do not have well aligned axes. The multiple field-cooling results presented here can be used to construct estimates for what might be expected from polycrystalline grain samples by averaging over a distribution of H_E values.

In summary, we have studied the angular dependence of the bias field in an exchange-coupled ferromagnet/antiferromagnet bilayer. We have shown that the spin structure at the interface plays a major role in determining the complexity of the bias field as a function of the applied field angle $H_E(\theta_H)$. Canting of the interfacial antiferromagnet spins, similar to the behavior found in an antiferromagnetic spin-flop configuration, results in a more complicated angular dependence for the bias field. In particular, the presence of interfacial line and step defects bifurcates the unidirectional axis of exchange-bias, with the equilibrium orientation or ''natural angle'' of the ferromagnetic spins governing the direction of that axis. Phase shifts in the sinusoidal functional form of $H_E(\theta_H)$ were found to be related to the natural angle. The sense of rotation of the ferromagnetic layer during reversal was found to cause a discontinuity in $H_E(\theta_H)$.

ACKNOWLEDGMENTS

The authors would like to thank L. Wee for stimulating and fruitful discussions. R.L.S. was supported by an ARC Grant. The work of R.E.C. and B.V.M. was supported by ARO Grant Nos. DAAG55-98-0294 and DAAH04-94-G-0253.

[1] B. Dieny, V. S. Speriosu, S. S. P. Parkin, B. A. Gurney, D. R. Wilhoit, and D. Mauri, Phys. Rev. B **43**, 1297 (1991).
[2] For a recent review, see J. Nogués and Ivan K. Schuller, J. Magn. Magn. Mater. **192**, 203 (1999).
[3] J. W. Cai, K. Liu, and C. L. Chien, Phys. Rev. B **60**, 72 (1999).
[4] J. Nogués, D. Lederman, T. J. Moran, and Ivan K. Schuller, Phys. Rev. Lett. **76**, 4624 (1996).
[5] J. Nogués, D. Lederman, T. J. Moran, and Ivan K. Schuller, Appl. Phys. Lett. **68**, 3186 (1996).
[6] W. P. Meiklejohn and C. P. Bean, Phys. Rev. **102**, 1413 (1956).
[7] W. P. Meiklejohn and C. P. Bean, Phys. Rev. **105**, 904 (1957).
[8] C. Tsang, N. Heiman, and K. Lee, J. Appl. Phys. **52**, 2471 (1981).
[9] A. P. Malozemoff, Phys. Rev. B **35**, 3679 (1987).
[10] D. Mauri, H. C. Siegmann, P. S. Bagus, and E. Kay, J. Appl. Phys. **62**, 3047 (1987).
[11] L. Néel and N. Kurti, *Selected Works of Louis Néel* (Gordon and Breach, New York, 1988).
[12] N. C. Koon, Phys. Rev. Lett. **78**, 4865 (1997).
[13] O. Allegranza and M.-M. Chen, J. Appl. Phys. **73**, 6218 (1993).
[14] R. Jungblut, R. Coehoorn, M. T. Johnson, Ch. Sauer, P. J. van der Zaag, A. R. Ball, Th. G. S. M. Rijks, J. aan de Stegge, and A. Reinders, J. Magn. Magn. Mater. **148**, 300 (1995).
[15] T. Ambrose, R. L. Sommer, and C.L. Chien, Phys. Rev. B **56**, 83 (1997).
[16] T. Mewes, Diploma Thesis, Universität Kaiserslautern, 1998.
[17] Y. J. Tang, B. F. P. Roos, T. Mewes, A. R. Frank, M. Rickart, M. Scheib, M. Bauer, S. O. Demokritov, and B. Hillebrands (unpublished).
[18] X. W. Wu, T. Ambrose, and C. L. Chien, Appl. Phys. Lett. **72**, 2176 (1998).
[19] D. V. Dimitrov, Shufeng Zhang, J. Q. Xiao, G. C. Hadjipanayis, and C. Prados, Phys. Rev. B **58**, 12 090 (1998).
[20] M. D. Stiles and R. D. McMichael, Phys. Rev. B **59**, 3722 (1999).
[21] R. L. Stamps (unpublished).
[22] B. V. McGrath, R. E. Camley, Leonard Wee, Joo-Von Kim, and R. L. Stamps (unpublished).
[23] R. E. Camley, B. V. McGrath, R. J. Astalos, R. L. Stamps, and Joo-Von Kim, J. Vac. Sci. Technol. A **17**, 1335 (1999).